NIH Public Access
Author Manuscript
Am J Hematol. Author manuscript; available in PMC 2016 March 01.

Published in final edited form as:
Am J Hematol. 2015 March ; 90(3): 235–241. doi:10.1002/ajh.23920.

Abnormal erythroid maturation leads to microcytic anemia in the TSAP6/*Steap3* null mouse model

Lionel Blanc, PhD[1,#,*], **Julien Papoin, MS**[1,*], **Gargi Debnath, PhD**[1], **Michel Vidal, PhD**[2], **Robert Amson, MD**[3], **Adam Telerman, MD, PhD**[3], **Xiuli An, MD, PhD**[1], and **Narla Mohandas, DsC**[1]

[1]Red Cell Physiology Lab, New York Blood Center, New York, NY 10065

[2]DIMNP UMR 5235, Montpellier, France 34090

[3]Institut Gustave Roussy, U981, Villejuif, France 94805

Abstract

Genetic ablation of the ferrireductase STEAP3, also known as TSAP6, leads to severe microcytic and hypochromic red cells with moderate anemia in the mouse. However, the mechanism leading to anemia is poorly understood. Previous results indicate that TSAP6/*Steap3* is a regulator of exosome secretion. Using TSAP6/*Steap3* knockout mice, we first undertook a comprehensive hematologic characterization of the red cell compartment, and confirmed a dramatic decrease in the volume and hemoglobin content of these erythrocytes. We observed marked anisocytosis as well as the presence of fragmenting erythrocytes. Consistent with these observations, we found by ektacytometry decreased membrane mechanical stability of knockout red cells. However, we were unable to document significant changes in the expression levels of the major skeletal and transmembrane proteins to account for this decrease in the membrane stability. Furthermore, there were no differences in red cell survival between wild type and knockout animals. However, when we monitored erythropoiesis, we found a decreased number of proerythroblasts in the bone marrow of TSAP6/*Steap3*$^{-/-}$ animals. In addition, progression from the proerythroblastic to the orthochromatic stage was affected, with accumulation of cells at the polychromatic stage. Altogether, our findings demonstrate that abnormal erythroid maturation is the main cause of anemia in these mice.

Keywords

hematologic diseases; iron deficiency; dyserythropoiesis; erythrocyte indices; erythrocyte membrane

Correspondence: Lionel Blanc, PhD, Laboratory of Developmental Erythropoiesis, The Feinstein Institute for Medical Research, 350 Community Drive, Manhasset NY 11030 USA, Phone: (516)-562-1507, Fax: (515)-562-1599, Lblanc@nshs.edu.
[#]Present address: The Feinstein Institute for Medical Research, Manhasset, NY 11030
[*]These authors contributed equally to this work

Authorship
L.B. and J.P. designed and performed research, analyzed data and wrote the manuscript; G.D. performed research and analyzed data; and M.V., R.A., A.T., X.A., and N.M. designed research, analyzed data, and edited the manuscript.

Conflict of interest disclosure
The authors declare no competing financial interests.

NIH-PA Author Manuscript
NIH-PA Author Manuscript
NIH-PA Author Manuscript

NIH-PA Author Manuscript

NIH-PA Author Manuscript

NIH-PA Author Manuscript

Introduction

During erythropoiesis, the differentiating red cell acquires properties that make it unique in terms of deformability and stability. At the membrane, two multi-protein complexes and underlying cytoskeleton are assembled, which allow the red cell to deform as it passes through the blood capillaries to deliver oxygen throughout the body [1]. In adult mammals, hemoglobin, which accounts for 90% of the total protein content of the red cell, consists of a heterotetramer composed of two alpha- and two beta-globin chains ($\alpha_2\beta_2$) non-covalently bound to a heme group. A charged atom of iron is at the center of the heme group, and is essential for the oxygen-carrying function of hemoglobin [2]. The iron used in hemoglobin synthesis comes from recycled iron.

In the circulation, oxidized iron (Fe(III)) is bound to transferrin (Tf). Once differic ($Fe(III)_2$) loaded-transferrin binds to its receptor (Transferrin Receptor-1, TfR1), subsequent endocytosis allows iron to be delivered to the endosomal compartment in the erythroblast [3]. During mammalian erythropoiesis, expression of TfR1 is finely regulated, and parallels hemoglobin synthesis. Its regulation has been the focus of numerous studies and involves, at least in part, sorting through the exosomal pathway [4–6]. After endocytosis, $Fe(III)_2$ is released from transferrin in the endosome upon acidification of the compartment. The coupled apo-transferrin/TfR1 is recycled back to the plasma membrane, and iron is delivered to the cytosol via the divalent metal transporter 1 (DMT1) [7, 8]. However, prior to its released into the cytosol, iron has to be reduced to Fe(II), a role achieved by a family of ferrireductases called STEAP (six-transmembrane epithelial antigen of prostate).

Studies by Fleming *et al.* on *nm1054*, a spontaneous mutation that arose in the mouse, allowed the identification of STEAP3 as the major ferrireductase in the erythroblast [9–11]. However, prior to the discovery of this mutant, STEAP3 had been named TSAP6 (Tumor Supressor Activated Pathway 6) after it had been found to play a role in cancer. Indeed, a series of studies identified *TSAP6* as a gene activated in tumor suppression and reversion after p53 activation [12–14]. In order to study the function of TSAP6/*Steap3*, we previously generated knockout mice, and found that these mice presented with a microcytic anemia along with a deregulation of TfR1 sorting and exosomal secretion [15]. However, the red cell phenotype had not been characterized in depth, and the mechanism leading to the microcytic anemia was unclear.

Here, using TSAP6/*Steap3* knockout mice as a model, we investigated the consequences of its ablation on the membrane stability of red blood cells and erythropoiesis. We undertook a comprehensive hematologic characterization of the red cell compartment, and showed that the microcytic, hypochromic anemia is characterized by a decrease in the membrane deformability, increased fragmentation and resistance to osmotic stress. However, none of the major transmembrane or cytoskeletal proteins were affected in their expression pattern, precluding a problem in the vertical or horizontal linkages. Furthermore, red cell survival was not compromised in knockout animals, but erythropoiesis was quantitatively affected, resulting in altered ratios of erythroblasts stages. Altogether, these results suggest that the microcytic anemia observed in TSAP6/*Steap3* null mice is predominantly due to abnormal erythropoiesis.

NIH-PA Author Manuscript

NIH-PA Author Manuscript

NIH-PA Author Manuscript

Methods

Mice

Generation of the TSAP6/*Steap3* null mice was described previously [15]. All studies were conducted on animals of at least 3 months of age, both male and female. Animal protocols were reviewed and approved by the New York Blood Center Animal Care and Use Committee.

Statistics

Data are presented as mean ± standard deviation, and differences between mean values were tested for significance using the two-tailed Student *t*-test.

Genotyping

Mice were genotyped as previously described [15], using the following primers:

F1 5'-GAGTGACCACCTCTCTCAGTCC-3',

R1 5'-AACACCGGTGACTACTGTGCTTTCG-3',

R2 5'-AAGGAACACTGTCTCCACCAGTCCC-3'.

TSAP6/*Steap3* knockout mice are defined as $tsap6^{\Delta 2-3}$. A typical result of the genotyping is presented in Supplemental Figure 1.

Antibodies

Mouse monoclonal anti-human transferrin receptor (TfR) was from Invitrogen. Mouse monoclonal anti-NHE-1, clone 4E9; and rabbit polyclonal anti-AQP-1 were from Millipore. Mouse monoclonal anti-β-Actin was from Sigma Aldrich. Rabbit polyclonal antibodies against spectrin, ankyrin, 4.1R, 4.2, 4.9, Band 3, Glycophorin A, Adducin and Tropomodulin-1 were generated in our laboratory. Peroxidase-conjugated donkey anti-rabbit IgG and sheep anti-mouse IgG were from Jackson ImmunoResearch Laboratories. Purified rat anti-mouse CD16/CD32, FITC-conjugated rat anti-mouse Ter119, APC-conjugated rat anti-mouse CD44, APC-Cy7-conjugated rat anti-mouse CD11b; CD45; and GR1 were from BD Pharmingen.

Automated cell counts

Whole blood was collected from the retroorbital sinus using EDTA-coated microhematocrit capillaries. Complete blood counts were obtained using an automated hematology analyzer (Advia 120 multispecies hematology analyzer, Bayer Healthcare).

Transmission electron microscopy

Red cells from wild type and TSAP6/*Steap3* knockout mice were fixed in 2% (vol/vol) glutaraldehyde in 0.1M sodium cacodylate (pH 7.4) for 1 hour at RT and washed three times in 0.1M sodium cacodylate (200g, 10min, RT). Fixed cells were stained with 2% (vol/vol) OsO_4 buffered in 0.1M sodium cacodylate (1 hour, RT). Samples were dehydrated using increasing concentrations of ethanol. Following dehydration, samples were incubated in

NIH-PA Author Manuscript

NIH-PA Author Manuscript

NIH-PA Author Manuscript

propylene oxide/epon resin (50:50) and in propylene oxide/epon resin (25:75) for 1 hour at RT each. Finally, samples were embedded in 100% epon resin overnight at 60°C. Specimens were sectioned on RMC MTX ultramicrotome using a Diatome diamond knife, and imaged on a FEI Tecnai 12 spirit TEM operated at 80 kV. All chemicals used for electron microscopy were from Electron Microscopy Sciences.

Osmotic fragility

Red cells were isolated from whole blood by centrifugation (400g, 5min, 4°C), and washed three times in PBS. Pellets were resuspended (50%, vol/vol) in normal saline solution (170 mM NaCl), and kept on ice. Fragility curve solutions were prepared by serial dilutions of a 290 mOsm osmotic fragility solution (145 mM NaCl; 8 mM Na_2HPO_4; 1 mM NaH_2PO_4). Cells were then diluted six times in normal saline, and 10 μL of these diluted cells were added to each assay tube. After incubation (20 min at RT), unlysed cells were pelleted (400g, 5 min, RT), and the supernatant was collected. Percent of lysis was determined by reading absorbance at 540nm.

Ektacytometry

Cellular deformability and membrane stability was assessed by two methods, based on the viscosity of the buffer in which the red cells were suspended. In the first approach (low viscosity), whole red cells were resuspended in 3% (wt/vol) polyvinylpyrrolidone (PVP), and exposed to an increased shear stress (0–150 dynes/cm^2). This process was detected as an increase in the deformability index (DI) as a function of the shear stress using an ektacytometer as previously described [16] and reflects cellular deformability. In the second approach (high viscosity), the cells were resuspended in 40% dextran (molecular weight= 40,000 kDa), and subjected to a constant applied shear stress of 750 dynes/cm^2 for 10min to measure membrane stability [17].

Density Gradients

Blood was washed three times in PBS-0.5% (wt/vol) Bovine Serum Albumin (BSA, Sigma Aldrich), 1 mM EDTA (Ethylene Diamine Tetra Acetate, Sigma Aldrich). Red cells were then layered on top of an OptiPrep™/PBS Density Gradient (1.083, 1.087, 1.091, 1.095, 1.100 g/mL), and ultracentrifuged at 141,000g for 30 min at RT (Beckman L7–65 Ultracentrifuge).

Western Blot

Red cell membrane fractions (Ghosts) were prepared as previously described [18]. Protein samples were solubilized in Laemmli buffer, and separated by SDS-polyacrylamide gel electrophoresis (SDS-PAGE) in 10% (wt/vol) polyacrylamide gels. After migration, samples were electrophoretically transferred to nitrocellulose membrane (BioRad). Membranes were subsequently blocked for 1 hour at RT in 4% (wt/vol) nonfat milk (BioRad), 1% (wt/vol) Bovine Serum Albumin (BSA, Sigma Aldrich), PBS-T (137 mM NaCl, 10 mM phosphate, pH7.4; 2.7 mM KCl; 0.1% Tween 20), and incubated with the indicated primary antibodies overnight at 4°C. After three washes in PBS-T, membranes were incubated with the secondary antibody [Horseradish Peroxidase (HRP) conjugated] for 1 hour at RT. Enhanced

NIH-PA Author Manuscript

NIH-PA Author Manuscript

NIH-PA Author Manuscript

chemiluminescence method (Pierce Chemical) was finally used to detect immunoreactive bands.

Flow cytometry

After collection of the bone marrow and spleen of wild type and TSAP6/*Steap3* null mice, erythropoiesis was monitored as previously described [19]. Briefly, for leukocyte depletion by negative selection, single cell suspensions from the bone marrow or spleen were incubated with mouse CD45 microbeads (Miltenyi Biotech) for 15 min on ice. After one wash in PBS-0.5% BSA, cells were subjected to magnetic separation using MACS-LS separation columns (Miltenyi Biotech) according to the manufacturer's instructions. Leukocyte-depleted cells were resuspended in PBS 0.5% BSA, and blocked with a rat anti-mouse CD16/CD32 for 15min on ice. After blocking, cells were stained by adding a cocktail of APC-Cy7-conjugated rat anti-mouse CD11b, APC-Cy7-conjugated rat anti-mouse CD45, APC-Cy7-conjugated rat anti-mouse GR1, APC-conjugated rat anti-mouse CD44, and FITC-conjugated rat anti-mouse Ter119 for 30 min ice in the dark. Cells were washed three times in PBS 0.5% BSA (200g, 5min, 4°C), and fluorescence was acquired on a FACS-Canto (Becton Dickinson). All data were subsequently analyzed using FlowJo v10.0.6 (Tree Star).

Red Cell Survival

Red cell survival in wild type and TSAP/*Steap3* null mice was evaluated as previously described [20]. Briefly, 30 mg/ml EZ-link sulfo-NHS-Biotin (Thermo Scientific) was injected in the tail vein of the mice. Blood was then collected once a week, and red cells were pelleted and stained with PE-conjugated Streptavidin (BD Pharmingen). After incubation (30 min at 4°C), cells were washed twice in PBS-0.5% BSA (200g, 5min, 4°C) and fluorescence was acquired on a FACS-Canto (Becton Dickinson).

Results

The microcytic, hypochromic anemia observed in TSAP6/*Steap3* null mice is associated with decreased deformability, increased fragmentation and reduced osmotic fragility of the red blood cells

Phase microscopy analyses of peripheral blood from TSAP6/*Steap3* knockout mice showed aberrant red blood cell morphology (Figure 1A). Specifically, we found that erythrocytes were heterogeneous in terms of size and shape, characteristics of anisocytosis. To gain further insights into the morphology of these red cells, we performed transmission electron microscopy. As shown in Figure 1B, one can clearly observe a decrease in both the size and volume of the red cells from TSAP6/*Steap3* knockout mice as well as the presence of small particles, reminiscent of fragmented or fragmenting erythrocytes (red arrows). In line with these results, the hematologic parameters obtained by automated blood counts (Table 1) showed a reduced mean corpuscular volume (MCV), decreased cell hemoglobin content (MCH) and a decreased mean cell hemoglobin concentration (MCHC), an increased red blood cell distribution width (RDW) and an elevated reticulocyte count. These parameters reflect a microcytic (reduced MCV), hypochromic (reduced MCHC) anemia. The

NIH-PA Author Manuscript

NIH-PA Author Manuscript

NIH-PA Author Manuscript

reticulocyte count is elevated, although moderately, and indicates that the anemia is proliferative.

We hypothesized that the red cell fragmentation was due to a decrease in membrane deformability. To test this hypothesis, we assessed red cell deformability by ektacytometry. Erythrocytes were resuspended in 3% (wt/vol) PVP-PBS, and subjected to increased shear stress (0–150 dynes/cm^2). In these conditions, red cells from TSAP6/*Steap3* knockout animals deformed significantly less than their wild type counterparts (Figure 1C) implying reduced cellular deformability. In addition, when these assays were performed in high viscosity conditions (40% [wt/vol] dextran), one can observe a fragmentation in the knockout samples, suggesting that these red blood cells possess decreased membrane mechanical stability (Figure 1D). Another approach to assess the alterations in red cell surface area to volume ratio is based on measuring osmotic fragility of cells. When we subjected erythrocytes to this test, we found that the 50% lysis for the TSAP6/*Steap3* knockout was 80 mOsm compared to 165 mOsm for the wild type (Figure 1E) implying decreased volume-to-surface area ratio. Finally, when we loaded red blood cells from wild type and knockout mice on top of a discontinuous density gradient, we found a different distribution of erythrocytes, with very light cells in the knockout only (Figure 1E). In accordance with an elevated reticulocyte count (Table 1), some of the cells found in the lighter fractions were reticulocytes, as measured by flow cytometry using thiazole orange (data not shown). However, this distribution is mainly a reflection of the decreased hemoglobin concentration of red cells in the TSAP6/*Steap3* knockout model.

The membrane defect is not due to a change in the expression levels of a major red cell membrane protein

In an attempt to understand the membrane defects described above, we measured the expression levels of major skeletal and transmembrane proteins, notably those usually affected in common red cell membrane disorders [21]. Coomassie blue staining of red cell membrane proteins (Figure 2A) indicate no major difference between wild type and knockout samples; although, we consistently found a band around 16kDa (black arrow), which may correspond to the globin chains in the TSAP6/*Steap3* knockout, as previously reported in a model of severe β-thalassemia [22]. In addition, when we performed western blot analyses of the major cytoskeletal components, namely spectrin, ankyrin, adducin, 4.1R, 4.2, 4.9, tropomodulin and actin, we found no differences in their expression levels (Figure 2B). On the other hand, the transmembrane proteins NHE-1 and CD71 were higher in the knockout compared to the wild type, in contrast to Band 3, Glycophorin A (GPA) and Aquaporin-1 (AQP-1) that did not display a differential expression. NHE-1 and CD71 are down regulated at the reticulocyte stage, and the higher expression levels may be explained by the higher reticulocyte count found in the knockout animals (Table 1). However, we found a similar expression pattern for the main skeletal and transmembrane proteins that are involved in red cell membrane disorders [23]. These data preclude disruption of the vertical or horizontal linkages as the etiology of the membrane defect.

NIH-PA Author Manuscript

NIH-PA Author Manuscript

NIH-PA Author Manuscript

Abnormal erythroid maturation is part of the underlying mechanism leading to the microcytic anemia

Anemia can be due to defects in the production or destruction of red blood cells. The membrane fragmentation observed in the red cells from knockout animals led us to investigate the possibility of a problem in red cell survival. To test this hypothesis, we labeled red blood cells with biotin, and followed their clearance over time as described [20]. We did not find any differences between wild type and TSAP6/*Steap3* knockout in terms of *in vivo* clearance (Figure 3). These data suggest that red cell survival is unaffected.

In our previous study [15], we found that the spleen of TSAP6/*Steap3* knockout animals was enlarged, with an expansion of the red pulp, reminiscent of stress erythropoiesis [24]. In order to confirm this hypothesis, we collected the spleen of both wild type and knockout mice. All mice were at least three months old, to avoid any physiologic splenic erythropoiesis that is encountered after birth (Mohandas N. and An X., unpublished data). After CD45 depletion, FACS analyses showed that only one main population remained in the wild type (Supplemental Figure 2A, left panel), while a second population was observed in the knockout (Supplemental Figure 2A, right panel). Moreover, when we used CD44 and Forward Scatter (FSC) as markers of terminal erythroid differentiation, we found that erythroid precursors were present only in the spleen of knockout mice (Supplemental Figure 2B, right panel), confirming stress erythropoiesis in these animals.

The main compartment for red cell production is the bone marrow, which has the capacity to double its erythroid output under stress conditions [19]. Therefore, in order to delineate the mechanism of anemia and quantify erythropoiesis in TSAP6/*Steap3* knockout mice, we collected the bone marrow from these animals, and used CD44 and FSC as markers of differentiation as we did for the spleen. After myeloid cell depletion and positive gating of the living erythroid cell population, two main populations are identified based on the morphological complexity of the cells (forward scatter versus side scatter, Figure 4A) in the bone marrow of both wild type and TSAP6/*Steap3* knockout mice. However, in the knockout animals, we found an increase in the $CD44^{hi}/FSC^{hi}$ population and a decrease in the $CD44^{low}/FSC^{low}$ population (Figure 4B). We expressed the six distinguishable erythroid populations based on their CD44 expression as a function of FSC, and then compared the wild type and TSAP6/*Steap3* for their size (Figure 4C). We found that each population had comparable sizes, up to the reticulocyte stage, where cells from knockout samples were smaller. These results suggest that the decreased size is a late, but continuous process, starting at the transition between the orthochromatic and reticulocyte stages, *i.e.* when enucleation takes place. We quantitated the proportion of erythroblasts at each distinct stage of maturation, and found a decrease in the amount of proerythroblasts in the knockout animals (Figure 4D). The progression towards orthochromatic erythroblasts was affected in the bone marrow of the TSAP6/*Steap3* knockout, and we found a ratio of 1:4:16:24 from the pro- to orthochromatic stage. Altogether, these results demonstrated that there is an increased production of precursors both in the spleen (Supplemental Figure 2) and bone marrow (Figure 4) of TSAP6/*Steap3* knockout mice. Moreover, a difference in size observed in mature red cells from knockout animals compared to wild type occurs at the transition between the orthochromatic and reticulocyte stages.

NIH-PA Author Manuscript

NIH-PA Author Manuscript

NIH-PA Author Manuscript

Discussion

In the present study, we provide a comprehensive hematologic characterization of TSAP6/*Steap3* knockout mice, focusing on the red cell compartment. We confirmed that knockout red cells display marked microcytosis and demonstrated that these cells are mechanically unstable, indicative of cell fragmentation. These results coupled with increased resistance to osmotic stress suggest the volume-to-surface area ratio is altered in TSAP6/*Steap3* knockout mice, a finding observed in iron deficiency and thalassemia [25, 26].

We could not link the membrane fragmentation defect observed to any of the major components of the two main protein complexes. Several studies have demonstrated the role played by reactive oxygen species (ROS) on the membrane stability and the survival of the red blood cell [27–29]. In addition, TSAP6/*Steap3* was identified first as a ferrireductase. One may suggest that its genetic ablation could lead to the accumulation of Fe(III), the oxidized form of iron, which would be deleterious for the erythrocyte. When we measured the ROS levels in the red cells, however, we did not find any differences between wild type and knockout samples (data not shown). Our transmission electron microscopy studies did not reveal any inclusions reminiscent of globin precipitates (Figure 1B). Further, the density gradients revealed very low density cell populations in knockout mice (Figure 1F), and we consistently found a band corresponding to the globin chains on the coomassie stained gels of red cell membrane proteins (Figure 2A). We propose that maturing erythroblasts cannot reduce Fe(III), and therefore, cannot make functional heme. The globin chains, nevertheless, are synthetized normally and accumulate. As a result, there is a defect in the hemoglobin synthesis in TSAP6/*Steap3* knockout mice. We suggest that the microcytic, hypochromic anemia observed in the TSAP6/*Steap3* knockout mouse model is linked to iron deficiency, as in the *nm1054* model [9], rather than a defect in the globin synthesis.

In order to assess the underlying mechanism of the anemia in TSAP6/*Steap3* knockout mice, we used our recently described method that enables the quantitation of distinct stages of terminal erythroid differentiation both in normal and pathological conditions. Based on the cell size and the expression levels of CD44, we found in wild type mice a ratio of 1:2:6:15 from proerythroblasts to orthochromatic erythroblasts. However, in the bone marrow of the TSAP6/*Steap3* knock out animals, we found a ratio of 1:4:16:24, reflecting a higher number of divisions (Figure 4). A similar proportion of 1:3.5 for proerythroblast:basophilic erythroblast was found in the $Hbb^{th1/th1}$mouse, a model of β-thalassemia intermedia [19, 30]. In the thalassemia model, the ratios normalize after the basophilic stage, which is likely due to erythroid precursor apoptosis [31]. In the TSAP6/*Steap3* model however, the number of polychromatophilic erythroblasts remains increased compared to the wild type. This raises the question of imbalance among proliferation, differentiation and apoptosis in the TSAP6/*Steap3* knockout model. In our previous study, we showed that in the spleen of the knockout animals, Ter119 positive cells were less prone to apoptosis after γ-irradiation than their wild type counterparts [15]. Furthermore, in the context of cancer, *TSAP6* knockdown has been shown to lead to the inhibition of apoptosis [13]. Therefore, we believe that the increased number of precursors can divide and differentiate, thereby producing more red cells with less hemoglobin. On the contrary, in the thalassemia model, many progenitors undergo apoptosis, and therefore lead to a reduced number of red cells produced. Taken together, our

NIH-PA Author Manuscript

NIH-PA Author Manuscript

NIH-PA Author Manuscript

observations in the knockout mice suggest the possibility that TSAP6/*Steap3* may play a role beyond its function as a ferrireductase. Alternatively, the loss of its TSAP6/Steap3 ferrireductase activity may influence erythroid differentiation by mechanisms independent of its effects on iron delivery from the plasma.

The red cells produced are smaller, but when we compared each progenitor population based on their size, we found that they were comparable up to the reticulocyte stage. Membrane remodeling is an integral part of erythropoiesis and occurs, for the most part, during the very late stages, namely during enucleation and reticulocyte maturation [32, 33]. The nucleus is extruded with a significant amount of plasma membrane, and the membrane remodeling follows with the removal of the endosomal compartment through the exosomal pathway [33]. It is therefore tempting to suggest that, in the knockout model, more membrane is partitioned with the nucleus than reticulocyte during its expulsion. This could explain the difference in size observed at the reticulocyte stage. Finally, the membrane fragmentation observed in mature red cells exacerbates size reduction.

In conclusion, our work expands previous studies that were performed on this knockout mouse model, and offers an explanation for the mechanism underlying the microcytic anemia. While TSAP6/*Steap3* null mice are phenotypically similar to some extent to murine models of thalassemia and congenital erythropoietic porphyria, presenting with microcytosis and decreased MCHC, their etiologies differ [31, 34]. Abnormal terminal erythroid differentiation appears to account for the anemia observed in our knockout mice, and suggests *Steap3* is functionally important in erythroid differentiation. Whether this function is entirely related to its properties as a ferrireductase remains to be determined; however our data in the knockout mice demonstrate a phenotype clearly distinct from deficient transferrin-mediated iron delivery. As nonsense mutations in the *TSAP6/STEAP3* gene [35] have been reported in patients with severe hypochromic anemia, future studies will be aimed at characterizing erythropoiesis in these patients (*e.g.* using CD34+ cells from peripheral blood) in order to investigate how our findings translate to human disease. Taken together, these results suggest that TSAP6/*Steap3* regulates mammalian erythropoiesis. We believe that our study has important implications in the fields of iron deficiency, red cell membrane biology and erythropoiesis.

Supplementary Material

Refer to Web version on PubMed Central for supplementary material.

Acknowledgments

This work was supported by grants from the National Institute of Health, USA (Grant DK26263 and DK32094 to N.M.) and by a grant from the French Government (ANR-09-BLAN-0292-01 to A.T, R.A and M.V).

References

1. Mohandas N, Gallagher PG. Red cell membrane: past, present, and future. Blood. 2008; 112:3939–3948. [PubMed: 18988878]
2. Ponka P. Tissue-specific regulation of iron metabolism and heme synthesis: distinct control mechanisms in erythroid cells. Blood. 1997; 89:1–25. [PubMed: 8978272]

NIH-PA Author Manuscript NIH-PA Author Manuscript NIH-PA Author Manuscript

3. Dautry-Varsat A. Receptor-mediated endocytosis: the intracellular journey of transferrin and its receptor. Biochimie. 1986; 68:375–381. [PubMed: 2874839]

4. Johnstone RM, Adam M, Hammond JR, et al. Vesicle formation during reticulocyte maturation. Association of plasma membrane activities with released vesicles (exosomes). J Biol Chem. 1987; 262:9412–9420. [PubMed: 3597417]

5. Pan BT, Johnstone RM. Fate of the transferrin receptor during maturation of sheep reticulocytes in vitro: selective externalization of the receptor. Cell. 1983; 33:967–978. [PubMed: 6307529]

6. Brugnara C, Kruskall MS, Johnstone RM. Membrane properties of erythrocytes in subjects undergoing multiple blood donations with or without recombinant erythropoietin. British journal of haematology. 1993; 84:118–130. [PubMed: 8393334]

7. Fleming MD, Trenor CC 3rd, Su MA, et al. Microcytic anaemia mice have a mutation in Nramp2, a candidate iron transporter gene. Nat Genet. 1997; 16:383–386. [PubMed: 9241278]

8. Gunshin H, Mackenzie B, Berger UV, et al. Cloning and characterization of a mammalian proton-coupled metal-ion transporter. Nature. 1997; 388:482–488. [PubMed: 9242408]

9. Ohgami RS, Campagna DR, Antiochos B, et al. nm1054: a spontaneous, recessive, hypochromic, microcytic anemia mutation in the mouse. Blood. 2005; 106:3625–3631. [PubMed: 15994289]

10. Ohgami RS, Campagna DR, Greer EL, et al. Identification of a ferrireductase required for efficient transferrin-dependent iron uptake in erythroid cells. Nat Genet. 2005; 37:1264–1269. [PubMed: 16227996]

11. Ohgami RS, Campagna DR, McDonald A, et al. The Steap proteins are metalloreductases. Blood. 2006; 108:1388–1394. [PubMed: 16609065]

12. Amson RB, Nemani M, Roperch JP, et al. Isolation of 10 differentially expressed cDNAs in p53-induced apoptosis: activation of the vertebrate homologue of the drosophila seven in absentia gene. Proceedings of the National Academy of Sciences of the United States of America. 1996; 93:3953–3957. [PubMed: 8632996]

13. Passer BJ, Nancy-Portebois V, Amzallag N, et al. The p53-inducible TSAP6 gene product regulates apoptosis and the cell cycle and interacts with Nix and the Myt1 kinase. Proceedings of the National Academy of Sciences of the United States of America. 2003; 100:2284–2289. [PubMed: 12606722]

14. Yu X, Harris SL, Levine AJ. The regulation of exosome secretion: a novel function of the p53 protein. Cancer Res. 2006; 66:4795–4801. [PubMed: 16651434]

15. Lespagnol A, Duflaut D, Beekman C, et al. Exosome secretion, including the DNA damage-induced p53-dependent secretory pathway, is severely compromised in TSAP6/Steap3-null mice. Cell Death Differ. 2008; 15:1723–1733. [PubMed: 18617898]

16. Mohandas N, Clark MR, Jacobs MS, et al. Analysis of factors regulating erythrocyte deformability. J Clin Invest. 1980; 66:563–573. [PubMed: 6156955]

17. Mohandas N, Clark MR, Health BP, et al. A technique to detect reduced mechanical stability of red cell membranes: relevance to elliptocytic disorders. Blood. 1982; 59:768–774. [PubMed: 7059678]

18. Salomao M, Zhang X, Yang Y, et al. Protein 4.1R-dependent multiprotein complex: new insights into the structural organization of the red blood cell membrane. Proceedings of the National Academy of Sciences of the United States of America. 2008; 105:8026–8031. [PubMed: 18524950]

19. Liu J, Zhang J, Ginzburg Y, et al. Quantitative analysis of murine terminal erythroid differentiation in vivo: novel method to study normal and disordered erythropoiesis. Blood. 2013; 121:e43–e49. [PubMed: 23287863]

20. Hoffmann-Fezer G, Mysliwietz J, Mortlbauer W, et al. Biotin labeling as an alternative nonradioactive approach to determination of red cell survival. Ann Hematol. 1993; 67:81–87. [PubMed: 8347734]

21. An X, Mohandas N. Disorders of red cell membrane. British journal of haematology. 2008; 141:367–375. [PubMed: 18341630]

22. Advani R, Rubin E, Mohandas N, et al. Oxidative red blood cell membrane injury in the pathophysiology of severe mouse beta-thalassemia. Blood. 1992; 79:1064–1067. [PubMed: 1737090]

NIH-PA Author Manuscript

NIH-PA Author Manuscript

NIH-PA Author Manuscript

23. Tse WT, Lux SE. Red blood cell membrane disorders. Br J Haematol. 1999; 104:2–13. [PubMed: 10027705]
24. Paulson RF, Shi L, Wu DC. Stress erythropoiesis: new signals and new stress progenitor cells. Curr Opin Hematol. 2011; 18:139–145. [PubMed: 21372709]
25. Giacca S, Negrini AC. on the Peculiar Behavior of the Osmotic Resistance of Erythrocytes Using the Parpart-Dacie Method in Hypochromic Iron-Deficiency Anemia. Haematologica. 1963; 48:477–482. [PubMed: 14123800]
26. Schrier SL, Rachmilewitz E, Mohandas N. Cellular and membrane properties of alpha and beta thalassemic erythrocytes are different: implication for differences in clinical manifestations. Blood. 1989; 74:2194–2202. [PubMed: 2804358]
27. Friedman JS, Rebel VI, Derby R, et al. Absence of mitochondrial superoxide dismutase results in a murine hemolytic anemia responsive to therapy with a catalytic antioxidant. J Exp Med. 2001; 193:925–934. [PubMed: 11304553]
28. Johnson RM, Goyette G Jr, Ravindranath Y, et al. Hemoglobin autoxidation and regulation of endogenous H2O2 levels in erythrocytes. Free Radic Biol Med. 2005; 39:1407–1417. [PubMed: 16274876]
29. Winterbourn CC. Oxidative denaturation in congenital hemolytic anemias: the unstable hemoglobins. Semin Hematol. 1990; 27:41–50. [PubMed: 2405495]
30. Ginzburg YZ, Rybicki AC, Suzuka SM, et al. Exogenous iron increases hemoglobin in beta-thalassemic mice. Exp Hematol. 2009; 37:172–183. [PubMed: 19059700]
31. Ginzburg Y, Rivella S. beta-thalassemia: a model for elucidating the dynamic regulation of ineffective erythropoiesis and iron metabolism. Blood. 2011; 118:4321–4330. [PubMed: 21768301]
32. An X, Mohandas N. Erythroblastic islands, terminal erythroid differentiation and reticulocyte maturation. Int J Hematol. 2011; 93:139–143. [PubMed: 21293952]
33. Blanc L, Vidal M. Reticulocyte membrane remodeling: contribution of the exosome pathway. Curr Opin Hematol. 2010; 17:177–183. [PubMed: 20173636]
34. Bishop DF, Clavero S, Mohandas N, et al. Congenital erythropoietic porphyria: characterization of murine models of the severe common (C73R/C73R) and later-onset genotypes. Molecular medicine. 2011; 17:748–756. [PubMed: 21365124]
35. Grandchamp B, Hetet G, Kannengiesser C, et al. A novel type of congenital hypochromic anemia associated with a nonsense mutation in the STEAP3/TSAP6 gene. Blood. 2011; 118:6660–6666. [PubMed: 22031863]

NIH-PA Author Manuscript
NIH-PA Author Manuscript
NIH-PA Author Manuscript

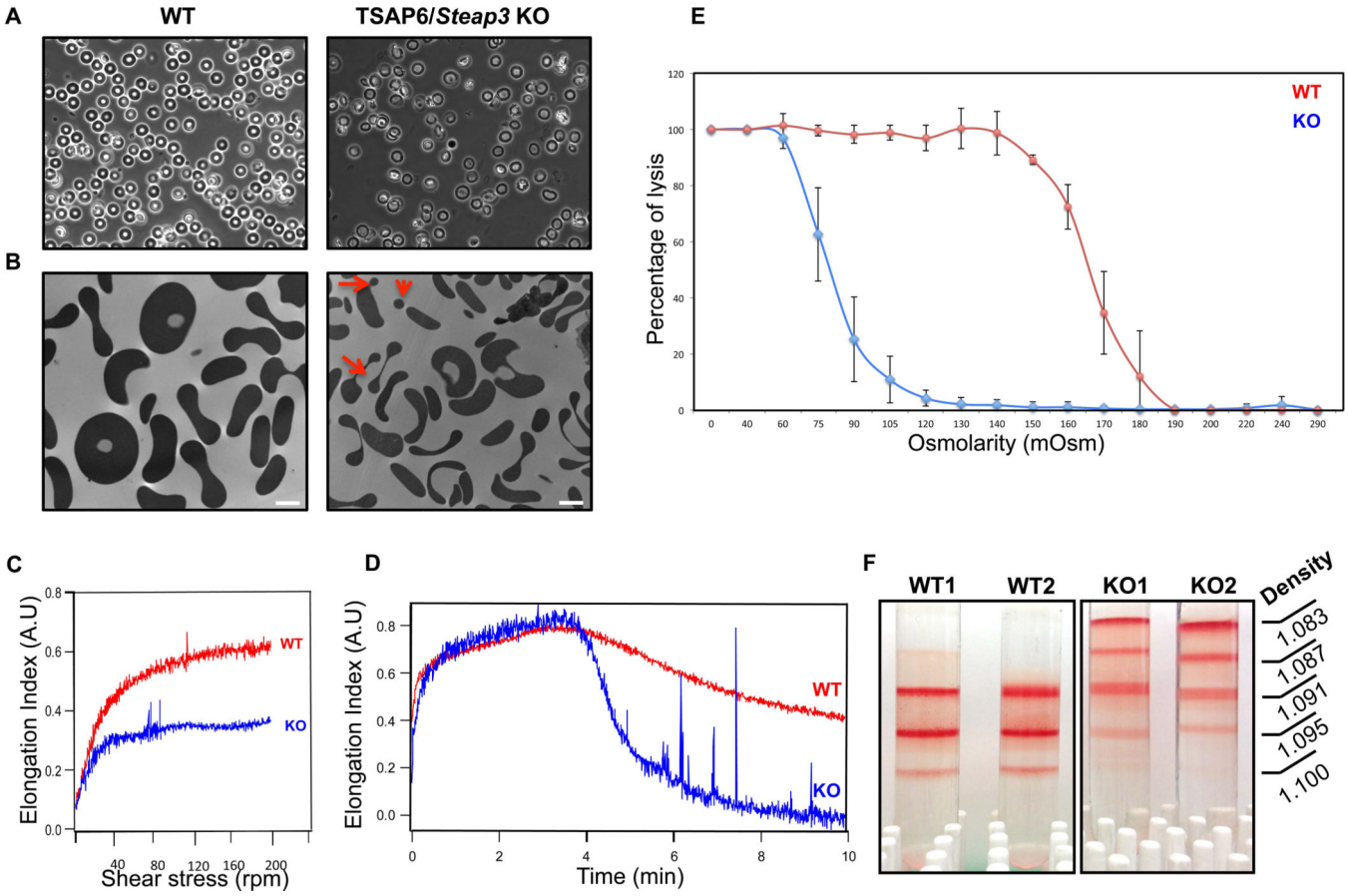

Figure 1. Phenotype of red cells from TSAP6/*Steap3* KO mice

(A) Phase contrast microscopy of peripheral blood from wild type (left panel) or TSAP6/*Steap3* knockout mice (right panel) shows heterogeneity in the shape of the red blood cells. (B) This is confirmed by transmission electron microscopy, where fragmentation of erythrocytes is apparent (red arrows). In addition, cells are smaller. Bar represents 2 μm. (C–D) Membrane deformability assessments by ektacytometry in 3% PVP (C) or 40% dextran (D) show reduced deformability for TSAP6/*Steap3* KO red blood cells. (E) Osmotic fragility is also reduced in knockout animals. Data presented X ± Standard deviation, n=4 in each group. All animals were 4 months of age. (F) Density gradients performed on red cells show a different density distribution in the knockout samples.

NIH-PA Author Manuscript
NIH-PA Author Manuscript
NIH-PA Author Manuscript

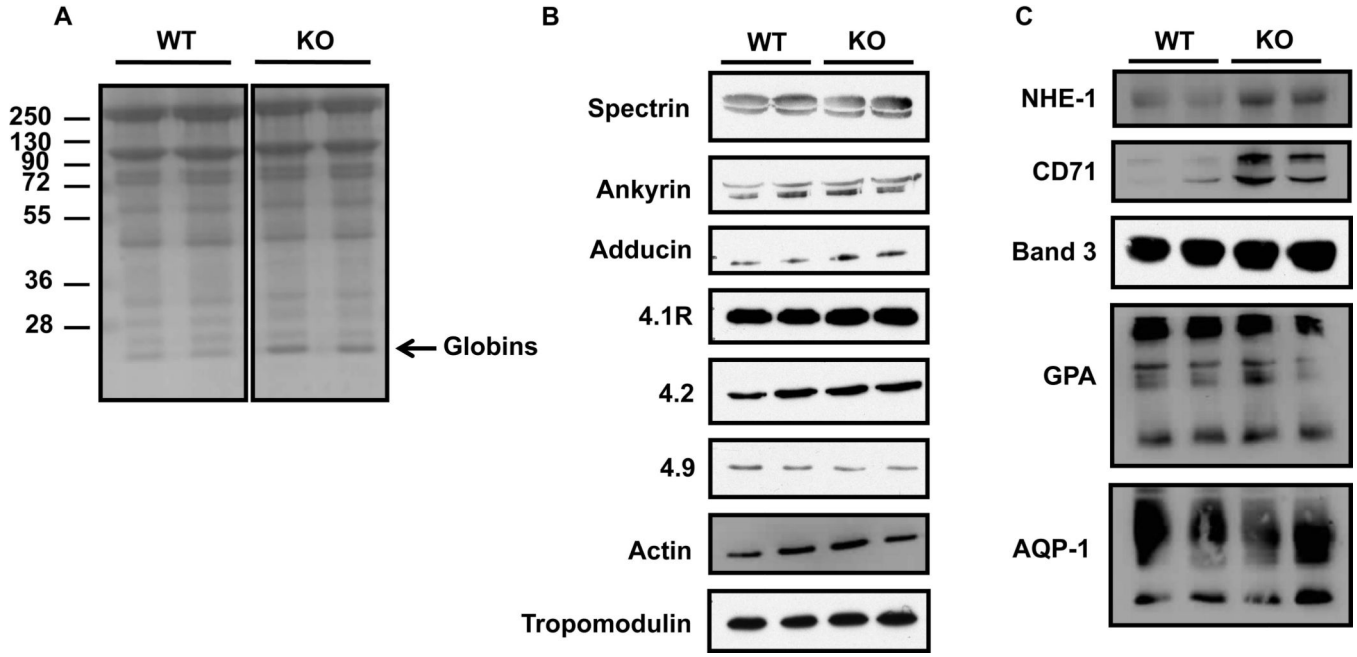

Figure 2. Expression levels of major red cell membrane proteins

(A) Coomassie blue staining of SDS-PAGE gel of red cell membranes (ghosts) shows no major differences between wild type and *Steap3* KO mice in terms of total protein contents. (B–C) Western blot analyses performed on ghosts from 2 wild type and 2 TSAP6/*Steap3* KO mice for cytoskeleton proteins (B) or transmembrane proteins (C). Only NHE-1 and CD71 expression levels were increased in ghosts from KO animals.

NIH-PA Author Manuscript
NIH-PA Author Manuscript
NIH-PA Author Manuscript

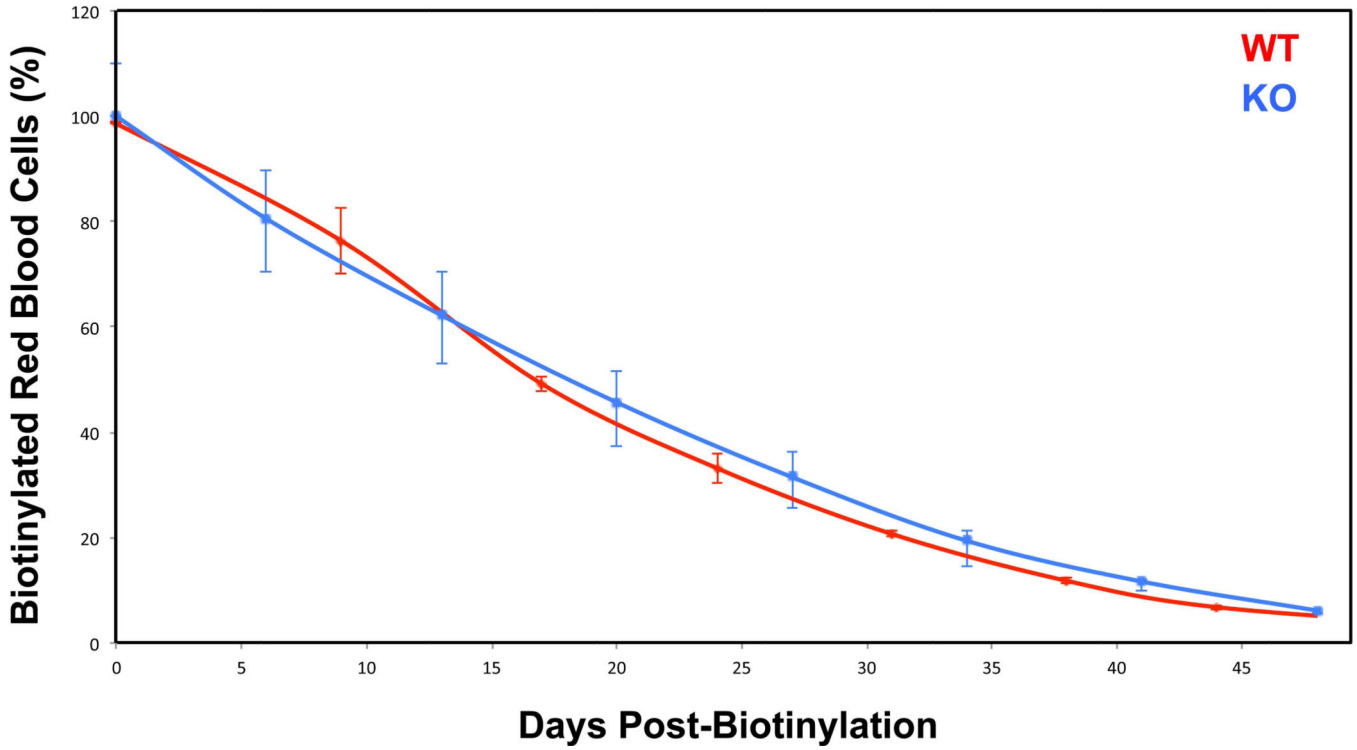

Figure 3. Red cell survival

Red cell lifespan was followed after biotin injections at day 0, and measured as a decrease in the amount of biotinylated red blood cells over time. There was no significant difference between wild type and TSAP6/*Steap3* knockout animals. Data presented X ± Standard Deviation, n=3 in each group. All animals were 4 months of age.

NIH-PA Author Manuscript
NIH-PA Author Manuscript
NIH-PA Author Manuscript

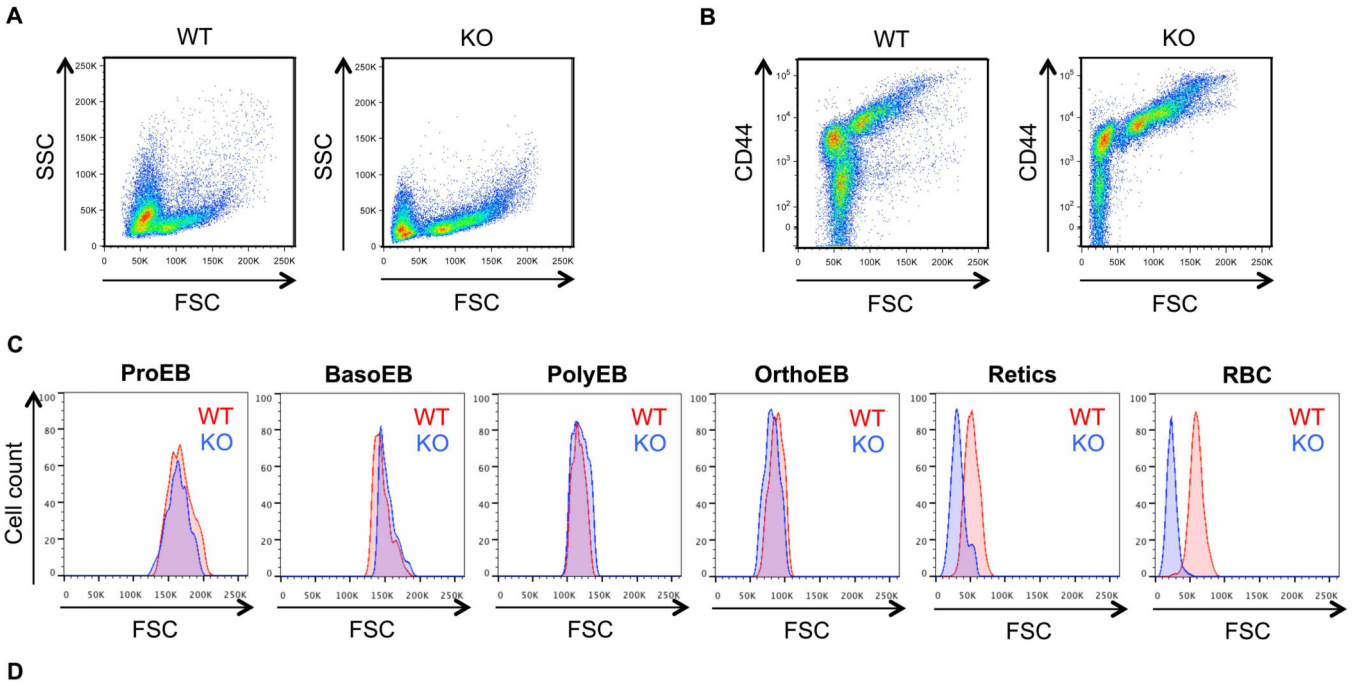

	ProEB (%)	BasoEB (%)	PolyEB (%)	OrthoEB (%)
Wild Type (n=5)	4.07 ± 0.77	9.18 ± 1.42	24.43 ± 2.05	62.30 ± 3.04
TSAP6/*Steap3* KO (n=5)	2.20 ± 0.49 **	9.03 ± 1.15	33.93 ± 2.12 ***	54.84 ± 3.48 **

Figure 4. Analysis of bone marrow erythropoiesis

(A) Bone marrow from WT and TSAP6 KO animals were collected and CD45 depletion was performed as described in Material and Methods. Representative pattern obtained after depletion, forward scatter (FSC) versus side scatter (SSC). (B) CD44 versus FSC plots demonstrate increased numbers of precursors ($CD44^{hi}/FSC^{hi}$) in the KO animals (right panels). (C) Analyses and comparisons of the size of each distinguishable population between wild type and TSAP6/*Steap3* knockout mice demonstrate that the loss of surface area appears after the orthochromatic stage (OrthoEB). (D) Quantification of the four distinct erythroblastic populations. Data presented X ± Standard deviation, n=5 in each group. $^{**}P \leq 0.01$ *vs* wild type; $^{***}P \leq 0.001$ *vs* wild type. All animals were 4 months of age. The proportion of erythroblasts at each stage was normalized to the total number of nucleated erythroblasts.

NIH-PA Author Manuscript

NIH-PA Author Manuscript

NIH-PA Author Manuscript

Table 1

Hematologic parameters

	RBC ($\times 10^6/\mu L$)	HGB (g/dL)	HCT (%)	MCV (fL)	MCH (pg)	MCHC (g/dL)	CH (pg)	RDW (%)	Retics (%)	Abs Retics ($\times 10^6/\mu L$)
Wild Type	9.5 ± 0.6	13.9 ± 0.6	43.3 ± 6.0	45.2 ± 3.6	14.5 ± 0.3	32.3 ± 3.1	13.9 ± 0.4	13.8 ± 0.8	2.6 ± 1.0	0.3 ± 0.1
TSAP6 KO	15.9 ± 1.2***	9.2 ± 0.9***	34.3 ± 6.4*	21.5 ± 3.2***	5.8 ± 0.3***	27.2 ± 2.8**	5.7 ± 0.2***	27.2 ± 2.2***	5.7 ± 3.0*	0.9 ± 0.4*

Data presented X ± SD, n=6 in each group.

* $P \leq 0.05$ *vs* wild type;

** $P \leq 0.01$ *vs* wild type;

*** $P \leq 0.001$ *vs* wild type.

All animals were at least 4 months of age.

RBC: Red Blood Cells; HGB: hemoglobin; HCT: Hematocrit; MCV: Mean Corpuscular Volume; MCH: Mean Corpuscular Hemoglobin; MCHC: Mean Cell Hemoglobin Concentration; CH: Corpuscular Hemoglobin; RDW: Red cell Distribution Width; Retics: Reticulocyte count; Abs Retic: Absolute Reticulocyte Count.